# Analyst

Accepted Manuscript






ROYAL SOCIETY OF CHEMISTRY

www.rsc.org/analyst

Analyst

RSCPublishing

PAPER

# Colorimetric and ratiometric pH responses by the protonation of phenolate within hemicyanine

Cite this: DOI: 10.1039/x0xx00000x

Jia-Tao Miao,[a] Chen Fan,[b] Xiao-Yu Shi,[a] Ru Sun,[*a] Yu-Jie Xu[b] and Jian-Feng Ge[*a,c]

Received 00th January 2012,
Accepted 00th January 2012

DOI: 10.1039/x0xx00000x

www.rsc.org/

Comparing with large amounts of nitrogen-reaction based pH optical responsible compounds, oxygen-reaction related pH sensors are less concerned. In this paper, the hemicyanine based pH probes are designed by the equilibrium between phenolate and phenol, and their reversible absorption and emission responses towards pH were evaluated. The indolium-phenol based tetramethylene hemicyanine (**1a**) has colorimetric response at 455 and 578 nm by the protonating and deprotonating processes, its emission spectra shows ratiometric changes at 594 and 654 nm with large Stokes shifts under acidic condition (139 nm) and basic condition (76 nm). The bromide substituent of the hemicyanine (**1b**) has lower p$K_a$ value compared with unsubstituted hemicyanine (**1a**), which suggests that adjustable p$K_a$ can be achieved by the modification of electron withdrawing groups. The theoretical calculations based on density functional theory (DFT) were also used for the explanation of the optical properties. Moreover, the *in cellulo* fluorescence imaging shows that the hemicyanine (**1a**) can be used in the detection of intracellular pH levels.



## Introduction

pH plays an important role in environment, industry and biology, the optical detection of pH has been developed with low-cost miniaturized light sources and photodetectors.[1] Comparing with normal pH indicators, the fluorescent pH probes are attracted much attention since the fluorescent method gives more precise analysis results. Fluorophores such as fluorescein,[2] coumarin,[3] rhodamine[4-6] or rhosamine,[7] cyanine,[8-11] naphthalimide,[12, 13] BODIPY,[14, 15] nile blue/red[16] and so on were applied in the design of the pH probes.

The nitrogen atom based optical responsible reactions were widely used because of the combinable nature between the lone pair electron within nitrogen and proton, and the nitrogen containing pH probes were mainly focused on three types of design philosophies. Firstly, the reaction based pH probe was broadly used by the variation of conjugated system, for example, the ring-opening reaction of the rhodamine,[17] cyanine based protonation of the free amine groups,[18] and recently developed equilibrium between phenoxazine and phenoxazinium.[16, 19] Secondly, the orbital energies of the guest parts are greatly changed by the electron donating amino group and electron withdrawing ammonium group, the protonation of amino based structure was used to disconnect or connect the photoinduced electron transfer (PET) process with host and guest parts of the probes,[11] and this design philosophy was successfully applied in several fluorophores;[20, 21] And thirdly, some nitrogen based pH probes were developed by intramolecular charge transfer (ICT) mechanism, their optical changes can be performed by the variation of intramolecular electron redistribution.[22] Although some pH probes were found by oxygen-containing ring open reaction,[2] the pH probes designed by oxygen atom as reaction centre are less reported.[23-26] The protonation of phenolate give less orbital energy changes between phenolate and phenol since the oxygen anion and hydroxyl group are both electron-donating groups, related pH probes based on ICT mechanism were only prepared with BODIPY[14] and Schiff base compound[27] and other limited fluorophores.

Cyanine, which was discovered in nineteenth century, has attracted interest as functional dyes in material[28-31] and biological fields.[11, 20, 32-35] It has the disadvantage of limited Stokes shifts. So far, some aminoheptamethinecyanines were found to own large Stokes shifts (>100 nm)[36, 37] and they were widely used as special kinds of near-infrared (NIR) fluorophores in several applications for chemo sensors.[38] Hemicyanine is one of the subbranches of cyanine dyes, and hemicyanines with terminal phenol were recently reported in the design of chemo sensors. The 2, 4-dinitrobenzenesulfonyl hemicyanine compound was reported as a probe for biological thiols.[39] An acrylate group containing hemicyanine was severed as a ratiometric fluorescent probe for distinguishing cysteine

from other biothiols.[40] And an allyl carbonate group functionalized hemicyanine dye was recently reported as a ratiometric fluorescent probe for palladium.[41] The above examples have greatly expanded the application of the hemicyanine in the detection field, meanwhile, these chemo sensors are tested in neutral pH condition with buffer solution, the discussion of the pH influence of the related hemicyanines with terminal phenol is essential for their real application in optical sensors. In this paper, two colorimetric and ratiometric pH probes that responses by the protonation of phenolate within hemicyanine are reported.

## Results and discussion

### Design and synthesis

The π-bonded donor-acceptor (D-π-A) structure is frequently adopted to construct ICT fluorescent probes with large Stokes shifts.[3] In this work, two new fluorescent pH probes (**1a-b**) with D-π-A structures are designed by connecting indolium to phenol structural unit. The phenolic hydroxyl group is an electron donating group whereas the deprotonated form of phenolate is a much stronger donating group. The protonation and deprotonation between phenolate and phenol units will lead to the ICT changes inside the target molecules (Scheme 1), and optical activitable response can be detected with the variation of pH in solution. Terminal phenolic hydroxyl group was used to minimize the possible intramolecular reaction of *o*-hydroxyl group[42] and the longer conjugated tetramethylene double bonds could lead the red shift comparing with dimethylene structures.[43] Different substituents with hydrogen (**1a**) or bromide atom (**1b**) in the ortho position of phenol group are used to evaluate the adjustable p$K_a$ values of the probes.

Scheme 1 gives the synthetic route and the sensing mechanism of the target chemosensors (**1a-b**). Compound **5** [44] was synthesized by the alkylation of the 2,3,3-trimethylindole. The phenolic hydroxyl groups were firstly protected to avoid the side effect in the following Wittig reaction, compounds **2a-b** were obtained by reactions of hydroxybenzaldehyde or 3-bromo-4-hydroxybenzaldehyde with chloromethyl methyl ether, respectively. The aldehydes (**4a-b**) can be prepared by hydrosis of the products prepared from Wittig reaction. The final products (**1a-b**) were synthesized by the condensations of compounds **5** and **4a-b** in methanol with catalytic amounts of pyridine. To improve their water solubility, the chloride form of final products (**1a-b**) were obtained by ion exchange using the 717 anion exchange resin. The structures were fully characterized by $^1$H NMR, $^{13}$C NMR and HRMS analysis.

### Optical properties of the probes 1a-b towards pH

The absorption and fluorescence pH titration experiments of **1a-b** (10 μM) were performed in various disodium hydrogen phosphate-citric acid buffer solutions[45] containing 5% DMSO. With decrease of pH from 9.4 to 5.4, the absorbance peak at around 578 nm (Fig. 1a, ε = 61300 $M^{-1}cm^{-1}$) significantly

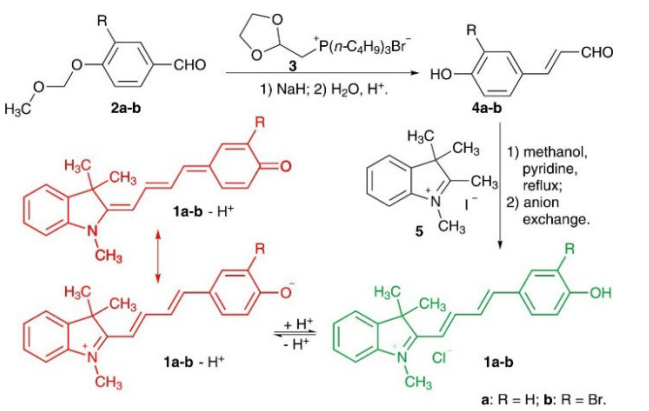


**Scheme 1** Synthesis of probes **1a**-**b** and their related deprotonated/protonated processes.

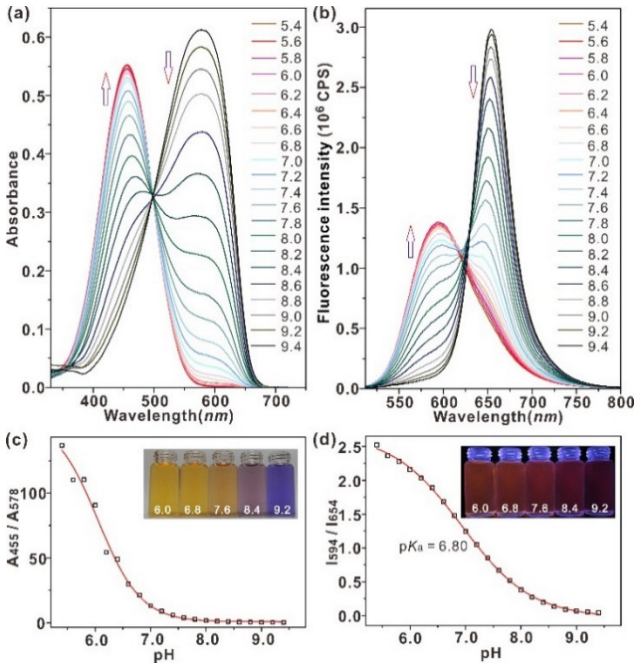


**Fig. 1** Optical responses of probe **1a** (10 μM) towards various pH values with disodium hydrogen phosphate-citric acid buffers containing 5% DMSO. (a) Absorption spectra. (b) Emission spectra ($\lambda_{ex}$ = 497 nm). (c) The absorption ratios $A_{455\ nm}/A_{578\ nm}$ towards different pH values, the inset is a pH-dependent photograph of the samples. (d) The emission ratios $I_{594\ nm}/I_{654\ nm}$ towards different pH values, the inset is a photograph under UV light ($\lambda_{ex}$ = 365 nm) in darkened room.

**Table 1.** Photochemical properties of pH probes **1a-b**

| Probe | pH | $\lambda_{abs}$[a] | $\lambda_{em}$[a] | ε ($M^{-1}\cdot cm^{-1}$) | Stokes shift[a] | Φ[b] |
|---|---|---|---|---|---|---|
| **1a** | 5.4[c] | 455 | 594 | $5.47\times10^4$ | 139 | 0.011 |
| | 5.4[d] | 453 | 594 | $4.69\times10^4$ | 141 | 0.008 |
| | 9.4[c] | 578 | 654 | $6.13\times10^4$ | 76 | 0.028 |
| | 9.4[d] | 573 | 653 | $5.04\times10^4$ | 80 | 0.022 |
| **1b** | 5.2[c] | 448 | 594 | $4.86\times10^4$ | 146 | 0.013 |
| | 8.2[c] | 558 | 659 | $5.44\times10^4$ | 101 | 0.039 |

[a] The absorption and emission maxima are using nm as units; [b] Cresyl violet was used as the reference. [c] The photochemical properties is measured in buffer containing 5% DMSO. [d] The photochemical properties is measured in buffer solution.

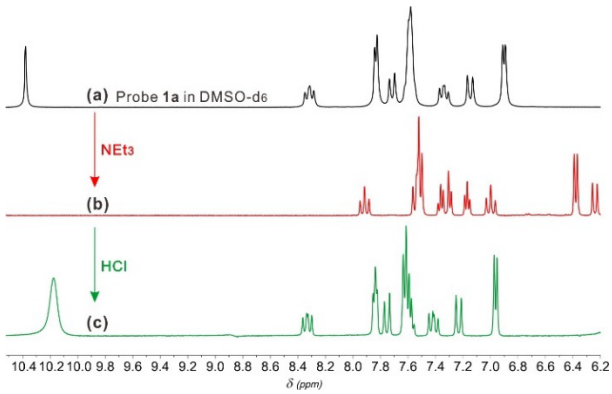


**Fig. 2** $^1$H NMR spectral deprotonated and protonated changes of probe **1a** in DMSO-$d_6$. (a) Probe **1a**. (b) Probe **1a** with 10 equiv. $Et_3N$. (c) Hydrochloric acid (20 equiv.) was added to the solution of (b).

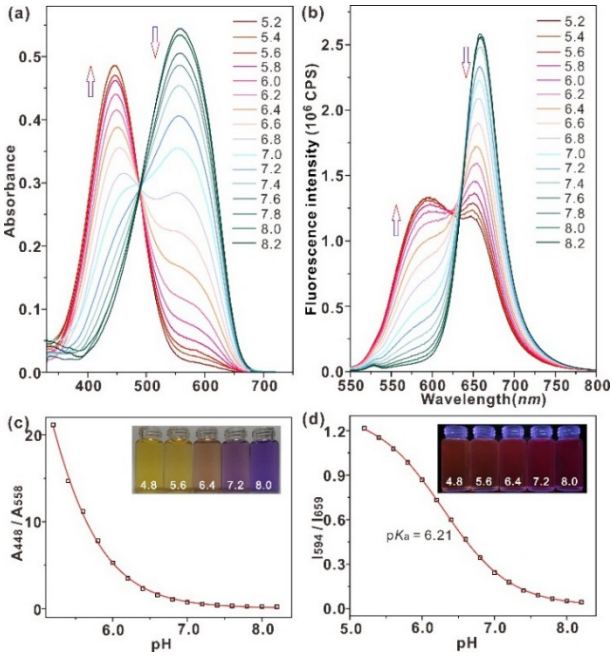


**Fig. 3** Optical responses of probe **1b** (10 μM) towards various pH values with disodium hydrogen phosphate-citric acid buffers containing 5% DMSO. (a) Absorption spectra. (b) Emission spectra ($\lambda_{ex}$ = 448 nm). (c) The absorption ratios $A_{448\ nm}/A_{558\ nm}$ towards different pH values, the inset is a pH-dependent photograph of the samples. (d) The emission ratios $I_{594\ nm}/I_{659\ nm}$ towards different pH values, the inset is a photograph under UV light ($\lambda_{ex}$ = 365 nm) in darkened room.

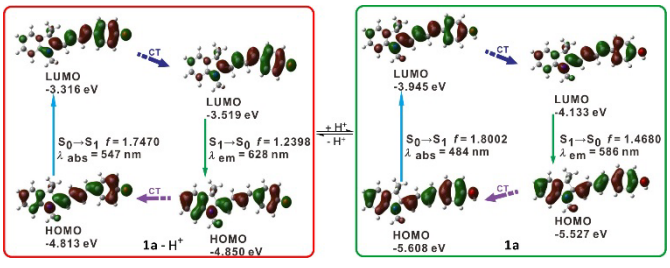


**Fig. 4** The frontier molecular orbitals (FMOs) involved in the vertical excitation and emission of probe **1a** in their deprotonated(left) and protonated(right) forms. CT stands for conformation transformation. Excitation and radiative processes are represented by solid lines and the nonradiative processes by dotted lines. For details please refer to Tables S2 and S3.

diminished, and a new blue-shifted absorption at 455 nm (Fig. 1a, ε = 54700 $M^{-1}cm^{-1}$) was formed simultaneously. There is a well-defined isobestic point at 497 nm in the absorption spectra. The fluorescence spectra of **1a** excited at 497 nm from pH 9.4 to 5.4 were recorded. In pH 9.4, probe **1a** exhibits only one emissive peak at 654 nm. With increasement of proton concentration, its fluorescence intensity at 654 nm was reduced and a new emission band at 594 nm emerged concomitantly (Fig. 1b). Indeed, ratiometric fluorescent measurement which uses the ratio of two fluorescent bands instead of the absolute intensity of one band, makes measuring the analyses more accurately and sensitively possible with minimization of the back-ground signal. The results that the blue-shift in the absorption and emission spectra with the decrease of pH may be explained by ICT changes in the basic and acidic conditions (Scheme 1 and TDDFT calculations below). To verify the detection mechanism, the protonating and deprotonating processes were characterized by $^1$H NMR spectra (Fig. 2), the low fields of $^1$H NMR was fully changed from **1a** (Fig. 2a) to the deprotonated structure (Fig. 2b), and all the peaks were reappeared in acidic condition (Fig. 2c). A p$K_a$ value of 6.80 was obtained using the plot of the fluorescence ratios $I_{594\ nm}/I_{654\ nm}$ (Fig. 1d).[46] Quantum yield measurements for probe **1a** at the pH extremes of 5.4 and 9.4 were 0.011 and 0.028 (Table 1), respectively. Further proof of the equilibrium was obtained by the observation of notable color changes from violet to yellow under visible light (Fig. 1c), and from royal purple to pink under ultraviolet light (Fig. 1d), when the pH decreased. Notably, probe **1a** has large Stokes shifts (139 nm at pH 5.4, 76 nm at pH 9.4). So the detection sensitivity can be improved by large Stokes shift because of the reduced self-quenching and minimized measurement errors.

The optical properties of probe **1b** were similar to the simplest compound **1a**. Due to the weak emission of acidic form of **1b** (Fig. S1), the excitation maximum of **1b** in pH 5.2 was selected as excited wavelength. As is shown in Fig. 3a-b, the absorption wavelength was blue-shifted 110 nm from 558 nm (pH=8.2) to 448 nm (pH=5.2) and a hypochromatic-shift by 65 nm from 659 nm (pH=8.2) to 594 nm (pH=5.2) in emission. Fluorescence quantum yields for probe **1b** at the pH extremes of 5.2 and 8.2 were 0.013 and 0.039 (Table 1), respectively. The color change of solution **1b** is a similar situation to **1a**. Color changes and isosbestic points formed in absorption and emission spectra indicate the equilibrium of two species. Homoplastically, probe **1b** also has very large Stokes shifts (146 nm at pH 5.2, 101 nm at pH 8.2). It is obviously indicated that the p$K_a$ of **1b** decreases to 6.21 when the electron-withdrawing bromine atom in the ortho position of the phenol was introduced (Fig. 3(d)).

## Rationalization of the optical properties of probes 1a-b with (TD)DFT calculations

Time-dependent density functional theory (TDDFT) has successfully been applied to study the optical properties of fluorescent dyes.[37, 47, 48] Zhou's group has systematically studied the effects of different functional on TD-DFT

calculations, and the results showed LSDA and BP86 functionals were closest to the experimental values.[49] Therefore, the UV-vis absorption (vertical excitation, Franck−Condon principle) and the emission properties of probes **1a-b** in their deprotonated/protonated forms were studied with TDDFT/BP86/TZVP calculations using the Gaussian program package.[50] The HOMO-LUMO gaps and the components of the transitions are listed in Table S1, S2 and S3, and the frontier molecular orbitals involved in the transitions are presented in Fig. 4 and Fig. S2.

The absorption and fluorescence pH titration experiments of probes **1a-b** have showed the blue-shifts both in the absorption band and in the emission spectra with the decrease of pH, which may be caused by the phenolate unit, a much stronger donating group, being replaced by the weaker donating group phenol unit, and that could be explained by weak ICT changes. Whereas, the intramolecular charge migration can be obviously observed from the FMOs plots of probes **1a-b** (Fig. 4 and S2), that is, the charge centers showing a slight shift to the phenolate unit after deprotonated. Moreover, the HOMO-LUMO gaps of probes **1a-b** in their protonated forms are much larger than the ones in their deprotonated forms for both $S_0$ and $S_1$ states (Table S1), which indicate that the theoretical results correlate well with the above experimental results. The detailed results of the absorption and emission spectra of probes **1a-b**, based on the TDDFT/BP86/TZVP/CPCM levels, are also in good agreement with the experimental data (Tables S2 and S3), which indicating BP86 functional is more suitable for the calculation of near infrared spectrum than B3LYP.[9]

**Reversibility, selectivity and aggregation assays of probes 1a-b**

It is well-known that the reversibility is highly required for monitoring reversible pH changes in living organs. When solutions containing the probes **1a-b** were changed to low or high pH, no noticeable changes in the emission ratios could be observed after five cycles (Fig. 5). This indicates that the stable optical properties of these probes make their potential application in real-time quantitative analysis of solution pH.

The selectivity of probes **1a** and **1b** for preferential binding to protons over other potential interferents under biological conditions was also investigated in acidic and basic conditions. As shown in Fig. 6 and Fig. S3, no noticeable changes was observed in the absorbance ratio and fluorescence intensity ratio of probes **1a** or **1b** (10 μM) in acidic or basic conditions in the presence of common cations, such as $K^+$, $Na^+$, $Ca^{2+}$ and $Mg^{2+}$, as well as heavy or transition-metal ions, such as $Cd^{2+}$, $Co^{2+}$,$Cu^{2+}$, $Hg^{2+}$, $Mn^{2+}$, $Ni^{2+}$. Moreover, bioactive amino acids, such as Lys, Phe, Gly, Glu, Arg, Cys, Pro, Try, and His, were also investigated, with no obvious changes observed. These results revealed that **1a** and **1b** showed an excellent selectivity response to pH in the presence of back-ground metal ions, bioactive amino acids as above described. Meanwhile，since cyanine dyes are prone to suffer the attack of nucleophiles, as is shown in Fig. S4, the fluorescence intensity does not change in disodium hydrogen phosphate -citric acid buffer buffer (7.4)

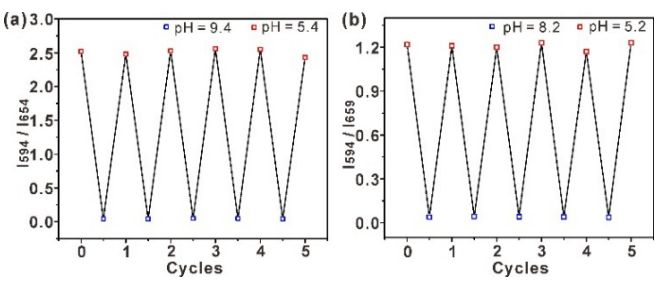


**Fig. 5** The reversible optical responses of probes **1a**-**b** between basic and acidic conditions. (a) The emission ratios ($I_{594\ nm}/I_{654\ nm}$) of probe **1a** at pH = 5.4 and 9.4. (b) The emission ratios ($I_{594nm}/I_{659\ nm}$) of probe **1b** at pH = 5.2 and 8.2.

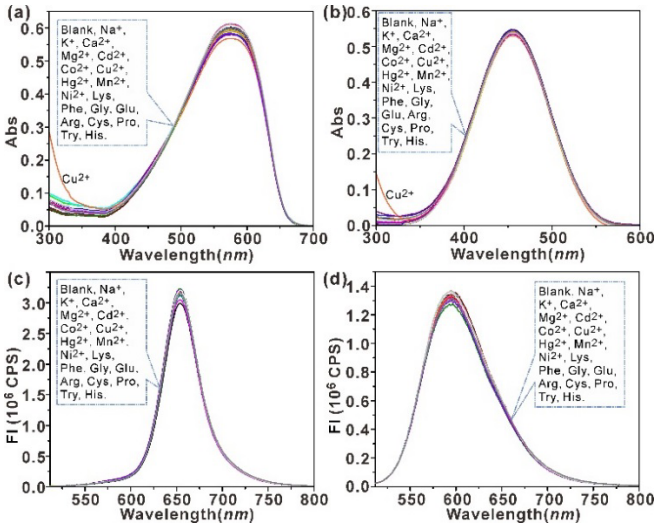


**Fig. 6** Optical responses of **1a** (10 μM) towards different analytes. (a, b) Absorption spectra. (c, d) Emission spectra. (a, c) Tested in basic buffer solutions with pH = 9.4. (b, d) Tested in acidic buffer solutions with pH = 5.4. Used analytes: $K^+$, $Na^+$ (100 mM); $Ca^{2+}$, $Mg^{2+}$(0.5 mM); $Cd^{2+}$, $Cu^{2+}$, $Co^{2+}$, $Hg^{2+}$, $Mn^{2+}$, $Ni^{2+}$ (0.3 mM); Cys, Phe, Gly, Glu, Arg, Lys, Pro, Try and His (0.1 mM).

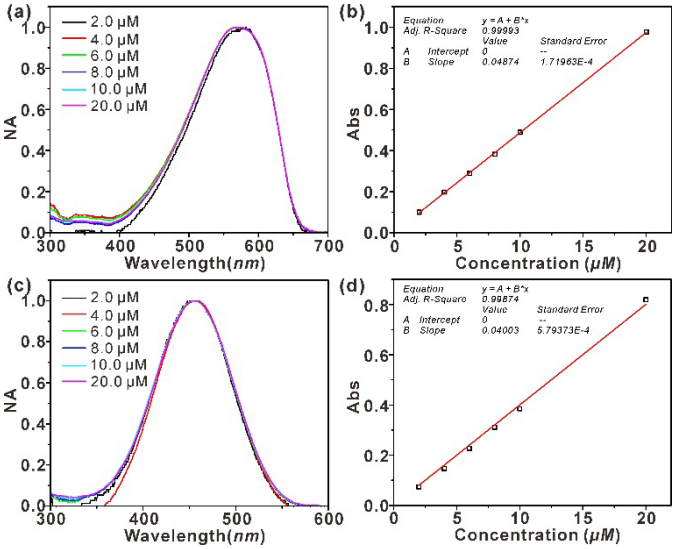


**Fig. 7** Concentration related absorptions of probe **1a** (2, 4, 6, 8, 10 and 20 μM) in basic and acidic conditions. (a, c) Normalized absorption spectra. (b, d) The linear relationship of absorption intensity and concentration. (a, b) Tested in basic buffer solutions with pH = 9.2. (c, d) Tested in acidic buffer solutions with pH = 4.8.

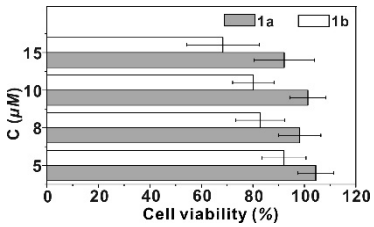


**Fig. 8** Percentages of HeLa cell viabilities remaining after cell treatment with probes **1a**-**b** (untreated cells were considered to have 100% survival). Cell viabilities were assayed by the MTT method.

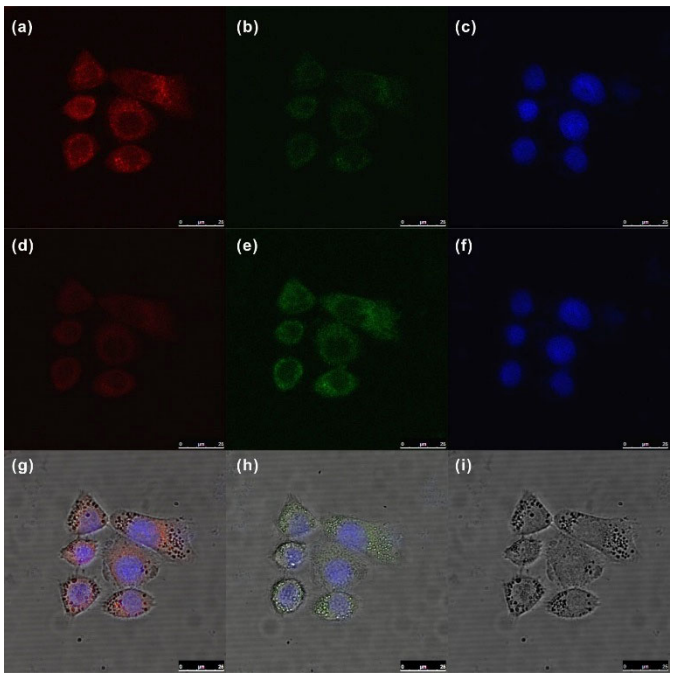


**Fig. 9** Fluorescence images of living HeLa cells with probe **1a** (8 μM) and Hoechst 33342. (a-c) Cells were treated with basic high $K^+$ buffer (pH = 8.0). (d-f). Cells were treated with acidic high $K^+$ buffer (pH = 6.0). (a-b, d-e) Fluorescent signals obtained from probe **1a**. (c, f) Fluorescent signals obtained from Hoechst 33342 which located in the nuclei. (g) Merged image of bright-field transmission image and (a-c). (h) Merged image of bright-field transmission image and (d-f). (i) Bright-field transmission image of HeLa Cells. (a, d) Red channels were collected in 650-750 nm with excitation at 488 nm. (b, e) green channels were collected in 530-590 nm with excitation at 488 nm. (c, f) Blue channels were collected in 410-480 nm with excitation at 405 nm.

containing 5% DMSO and 10% fetal bovine serum (FBS) for 36 h, which confirms that dye **1a** is stable enough in biological conditions.

Cyanine dyes tend to aggregate in solution, resulting in new peaks in their concentration-dependent normalized absorption spectra. Thus, the concentration-dependent optical properties of the probes **1a**-**b** were examined. As shown in Fig. 7, the absorption maxima of probe **1a** in acidic or basic conditions showed a linear dependence on concentration (2-20 μM). No obvious new peaks were observed in normalized absorption-concentration plots. Probe **1b** also shows the similar linear properties (Fig. S5).

### *In cellulo* application

A MTT-based colorimetric assay of compounds **1a**-**b** in HeLa cells was studied firstly. As it is shown in Fig. 8, after six hours of cellular internalization of the probe at a concentration of 8 μM, more than 98% cells were viable with **1a**, while only 82% cells were viable with **1b**. At high concentrations of 15 μM, the cell viability remains more than 90% with **1a** but less than 70% with **1b**. The results indicate the low-cytotoxicity of **1a**, which is one of the key criteria for living cell imaging. Then the probe **1a** is more suitable for fluorescence imaging pH fluctuations in live cells.

Laser scanning confocal microscopy of HeLa cells was used to characterize the pH imaging of the probe **1a**. Cells were first treated with the nuclear-specific Hoechst 33342 (50 nM) dye to co-stain the cells with probe **1a**, and the position of the nucleolus can be detected by the image obtained in the blue channel (excited at 405 nm, detected in 410–480 nm). Then, cells were incubated with **1a** (8 μM) for 20 min and washed twice with phosphate-buffered saline (PBS). To adjust the intracellular pH, cells were sequentially incubated with basic high $K^+$ buffer (pH = 8.0), acidic high $K^+$ buffer (pH = 6.0). Nigericin (2 $\mu g \cdot ml^{-1}$) was used to promote the acid-base balance between HeLa cells and their conditioned medium. As shown in Fig. 9, the images indicate that the emission of probe **1a** is distributed mainly in the cytoplasmic region. The **1a**-stained cells exhibited strong red fluorescence and weak green fluorescence when cell culture medium of high $K^+$ buffer at pH 8.0 was used (Fig. 9 (a,b)). When the pH of culture medium was decreased to 6.0, the fluorescence brightness obviously reduced in the red channel and increased in the green channel (Fig. 9 (d,e)). These above images demonstrated that **1a** could be employed for ratiometric imaging near-neutral pH fluctuations in live cells.

## Conclusions

The pH probes with oxygen based reaction center were designed in this paper, and the protonation and deprotonation processes between phenolate and phenol were adopted in hemicyanine based probes. Two D-π-A fluorescence pH probes have been successfully prepared by linking indolium to phenol structural unit. The indolium-phenol based tetramethylene hemicyanine (**1a**) has colorimetric response at 455 and 578 nm by the protonating and deprotonating processes, its emission spectra shows ratiometric changes at 594 and 654 nm with large Stokes shifts under acidic (139 nm) and basic (76 nm) conditions. The p$K_a$ values can be modified by the introduction of electron-withdrawing group in the ortho position of the phenol group. In particular, probe **1a** was well used for monitoring near-neutral pH fluctuations in live HeLa cells dues to its properties of low cytotoxicity, high selectivity, good reversibility, water solubility and membrane permeability.

## Experimental section

### Materials and Instruments

Starting materials and reagents (analytical grade) were purchased from TCI Development Co., Ltd. (Shanghai branch, China) or Sinopharm Chemical Reagent Co., Ltd. (Shanghai, China) and used directly. Chromatography was performed with silica gel (200-300 mesh). The buffer was made by disodium hydrogen phosphate (0.2 M) and citric acid (0.1 M) by the reported method.[45] Cresyl violet ($\Phi$ = 0.54, methanol) was used as the reference for fluorescence quantum yields in measurements, and the refractive index of the solvents are 1.44, 1.33 and 1.42[51] for methanol, water and water containing 5% DMSO (v/v) respectively.

Melting points were determined on an X-4 microscope electron thermal apparatus (Taike, China) and the values are uncorrected. $^1$H NMR and $^{13}$C NMR spectra were recorded on a Varian 400 MHz spectrometer. Mass spectra were tested on Finnigan MAT95 mass spectrometer. UV-vis absorption spectra were recorded on a Shimadzu U-3900 spectrometer. Fluorescence emission spectra were performed on a HORIBA Jobin Yvon FluoroMax-4 Spectrofluorometer. Fluorescence images of cells were obtained with a Leica TCS SP5 confocal fluorescence microscope. The pH values were measured with a Lei-Ci (pH-3C) digital pH-meter (Shanghai, China) using a combined glass-calomel electrode.

**Synthesis of compounds**

The compounds of **2a-b**,[52, 53] **3**[44] and **5**[54] were prepared according the reported procedures.

*3-(4-Hydroxyphenyl)acrylaldehyde* (**4a**). NaH (240 mg, 10 mmol) was added in one portion to a solution of aldehyde **2a** (332.0 mg, 2 mmol), **3** (886.0 mg, 2.4 mmol) and 18-crown-6 (c.a. 10mg) in dry THF (30 mL) under a $N_2$ atmosphere. After 10 h stirring at room temperature, the reaction mixture was quenched with water and extracted with ether. After removal of ether, the residue was dissolved in methanol (280 ml) and 3 M HCl (50 ml). After 1.5 h under reflux, the reaction mixture was poured into ice-water and extracted with $CH_2Cl_2$, and then the organic layer was dried over $Na_2SO_4$. After removal of solvents, the residue was purified by column chromatography (silica gel, petroleumether-ethyl acetate =4 : 1) to give compound **4a** as a pale yellow solid (189.6 mg, yield 64.0 %). Mp: 135.5-136.5 °C. $^1$H NMR (400 MHz, DMSO-$d_6$) δ 10.21 (s, 1H), 9.60 (d, $J$ = 7.9 Hz, 1H), 7.66 - 7.57 (m, 3H), 6.87 (d, $J$ = 8.6 Hz, 2H), 6.67 (dd, $J$ = 15.8, 7.9 Hz, 1H). $^{13}$C NMR (400 MHz, DMSO-$d_6$) δ 194.0, 160.6, 153.7, 131.0, 125.4, 125.2, 116.0. HRMS (ESI$^+$): m/z calcd for $[C_9H_9O_2]^+$: 149.0597, found 149.0593.

*3-(3-Bromo-4-hydroxyphenyl)acrylaldehyde* (**4b**). Compound **4b** was synthesized from **2b** and **3** in the same way as described in the synthesis of compound **4a**. A yellow solid, yield 61.0%, Mp: 136.8-137.8 °C. $^1$H NMR (400 MHz, DMSO-$d_6$) δ 11.03 (s, 1H), 9.59 (d, $J$ = 7.8 Hz, 1H), 7.95 (d, $J$ = 2.0 Hz, 1H), 7.60 (dd, $J$ = 8.9, 7.0 Hz, 2H), 7.02 (d, $J$ = 8.4 Hz, 1H), 6.74 (dd, $J$ = 15.8, 7.8 Hz, 1H). $^{13}$C NMR (101 MHz, DMSO-$d_6$) δ 194.0, 156.9, 152.1, 133.7, 129.7, 126.9, 126.7, 116.6, 110.1. HRMS (ESI$^+$): m/z calcd for $[C_9H_8BrO_2]^+$: 226.9702 and 228.9702, found 226.9710 and 228.9707.

*2-(4-(4-Hydroxyphenyl)buta-1,3-dien-1-yl)-1,3,3-trimethyl-3H-indol-1-ium chloride* (**1a**) To a mixture of **4a** (166.2 mg, 1.0 mmol) and **5** (301.2 mg, 1.0 mmol) in methanol (2.0 mL), pyridine (1 drop) was added, then the mixture was refluxed for 10 h. The reaction was cooled to room temperature, and the crude product was separated by filtration and the product was recrystallized from ethanol to give the iodide form of **1a**, then the methanol solution of the obtained iodide salt was passed through 717 anion exchange resin; the solvent was evaporated to obtain **1a** as a dark red solid (238.6 mg, yield 70.2 %). Mp: 159.7-161.8 °C. $^1$H NMR (400 MHz, DMSO-$d_6$) δ 10.38 (s, 1H), 8.41 – 8.23 (m, 1H), 7.83 (d, $J$ = 6.9 Hz, 2H), 7.72 (d, $J$ = 15.1 Hz, 1H), 7.59 (d, $J$ = 6.2 Hz, 4H), 7.34 (dd, $J$ = 14.6, 11.3 Hz, 1H), 7.15 (d, $J$ = 15.2 Hz, 1H), 6.90 (d, $J$ = 7.2 Hz, 2H), 3.97 (s, 3H), 1.97 – 1.50 (m, 6H). $^{13}$C NMR (101 MHz, DMSO-$d_6$) δ 180.7, 161.2, 155.6, 149.9, 143.1, 141.9, 130.8, 128.8, 128.6, 126.6, 125.7, 122.8, 116.5, 114.6, 114.0, 51.4, 33.7, 25.6. HRMS (ESI$^+$): m/z calcd for $[C_{21}H_{22}NO]^+$: 304.1696 , found 304.1683.

*2-(4-(3-Bromo-4-hydroxyphenyl)buta-1,3-dien-1-yl)-1,3,3-trimethyl-3H-indol-1-ium chloride*(**1b**). Compound **1b** was synthesized from **4b** and **5** in the same way as described in the synthesis of compound **1a**. A brown solid, yield 76.4 %. Mp: 155.5-157.5 °C. $^1$H NMR (400 MHz, DMSO-$d_6$) δ 11.17 (s, 1H), 8.29 (dd, $J$ = 15.3, 10.8 Hz, 1H), 7.90 (d, $J$ = 2.0 Hz, 1H), 7.88 – 7.80 (m, 2H), 7.66 – 7.52 (m, 4H), 7.40 (dd, $J$ = 15.2, 10.8 Hz, 1H), 7.17 (d, $J$ = 15.3 Hz, 1H), 7.06 (d, $J$ = 8.4 Hz, 1H), 3.98 (s, 3H), 1.73 (s, 6H). $^{13}$C NMR (101 MHz, DMSO-$d_6$) δ 180.8, 156.9, 154.5, 147.2, 143.2, 141.9, 132.8, 129.9, 128.9, 128.3, 127.1, 122.8, 117.0, 115.1, 114.8, 110.5, 51.6, 33.9, 25.4. HRMS (ESI$^+$): m/z calcd for $[C_{21}H_{21}BrNO]^+$: 382.0101 and 384.0101, found 382.0101 and 384.0784.

**Preparation of the test solutions**

Stock solutions (100 μM) of **1a-b** were prepared with DMSO-$H_2O$ (v:v=1:1). Each test solution (10 μM) was prepared in a volumetric flask (10 mL) from the corresponding stock solution (1.0 mL) and disodium hydrogen phosphate-citric acid buffer to give a total volume of 10 mL.

**Selectivity experiments**

Stock solutions of probes (100 μM) were prepared in a volumetric flask (100 mL) with DMSO (50.0 mL) and doubly distilled water. Stock solutions of various ions were prepared in volumetric flasks (10 mL) with concentrations of NaCl (1 M), KCl (1 M), $MgSO_4$ (5 mM), $CaCl_2$ (5 mM), $CoCl_2$ (3 mM), $CuCl_2$ (3 mM), $NiCl_2$ (3 mM) , $CdCl_2$ (3 mM), $HgCl_2$ (3 mM) in doubly distilled water. Stock solutions of all kinds of amino acids were all prepared in volumetric flasks (100 mL) with concentrations of 1 mM in doubly distilled water. Each test solution was prepared in a volumetric flask (10 mL) with 1 mL stock solution of probes and 1 mL stock solution of corresponding ions or amino acid solutions, diluted with disodium hydrogen phosphate-citric acid buffer solution.

**Cell culture and Imaging Methods**

HeLa cells were cultured in Roswell Park Memorial Institute culture medium (RPMI-1640) supplemented with 10% calf serum, penicillin (100 U·mL$^{-1}$), streptomycin (100 μg·mL$^{-1}$) and L-glutamine ($2.5 \times 10^{-4}$ M) at 37 °C in a 5:95 $CO_2$-air incubator. Cells with $2\times10^5$ density were loaded onto a glass-bottomed coverslip with a diameter of 35 mm and cultured for 48 h before use. Fluorescence images of cells were obtained with a Leica TCS SP5 confocal fluorescence microscope. Cells were first treated with the nuclear-specific Hoechst 33342 (50 nM). The blue channel was excited at 405 nm for the range of 410-480 nm. The green emission channel was excited at 488 nm and measured for the range 530-590 nm. The red emission channel of HeLa cells was excited at 488 nm and measured for the range 650-750 nm. Then, HeLa cells were incubated with probe **1a** (8 μM). After removing the nutrient fluid, phosphate-buffered saline (PBS) was used to wash the cells, and the basic high $K^+$ buffer (pH=8.0, 1.0 mL) with nigericin (2 μg·ml$^{-1}$) was added and cells were incubated for 10 min. The system was finally changed to acidic high $K^+$ buffer (pH=6.0, 1.0 mL) with nigericin (2 μg·ml$^{-1}$) and incubated for a further 10 min.

### MTT assay for the cell cytotoxicity

HeLa cell lines were seeded in 96-well microplates (Nunc, Denmark) at a density of 5-7 × $10^4$ cells per mL in 100 mL of medium for a stationary culture. After 24 h of cell attachment, the plates were washed with 100 mL per well PBS. Then different concentrations of probes **1a** and **1b** with 5 μM, 8 μM, 10 μM, 15 μM in fresh medium were added into the cell medium (1% DMSO) and incubated for 6 h. Cells in a culture medium without fluorescent dyes were used as the control. Six replicate wells were used for each control and tested concentrations. MTT solution (5 mg/mL, 10 mL) in PBS was subsequently added to each well. After incubation at 37 °C for 4 h in a 5% $CO_2$ humidified incubator, the remaining MTT solution was removed from wells and 150 mL of dimethysulfoxide (DMSO) was added into each well. The optimal density (OD) value was measured with a microplate reader at 490 nm wavelength. The cell viability was calculated as a percentage of the control culture value using the following formula: $(OD_{treated}/OD_{control}) \times 100\%$.

### Calculation details

The geometries of the probes **1a-b** in their deprotonated and protonated states at the ground state ($S_0$ state) were optimized by density functional theory (DFT) at the B3LYP/6-31+G(d) level, and the geometries at the lowest excited state ($S_1$ state) were optimized by TDDFT methods with the BP86/TZVP using the Gaussian program package. In some cases, higher excited states were optimized. There are no imaginary frequencies in frequency analysis of all calculated structures; therefore, each calculated structures are in local energy minimum. The energy gap between the $S_0$ state and the $S_1$ excited state was calculated with the (TD)DFT/BP86/TZVP method based on the optimized $S_0$ state geometry (for absorption) and the $S_1$ state geometry (for fluorescence), respectively. Water was used as the solvent for the (TD)DFT calculations (CPCM model).

### Acknowledgements

The project is supported from the National Natural Science Foundation of China (51273136) and the Project funded by the Priority Academic Program Development of Jiangsu Higher Education Institutions.

### Notes and references

[a] *College of Chemistry, Chemical Engineering and Material Science, Collaborative Innovation Center of Suzhou Nano Science and Technology, Soochow University, 199 Ren'Ai Road, Suzhou 215123, China. E-mail: sunru924@hotmail.com, ge_jianfeng@hotmail.com.*

[b] *School of Radiation Medicine and Protection, Medicine College of Soochow University, Suzhou 215123, China.*

[c] *Jiangsu Key Laboratory of Medical Optics, Suzhou Institute of Biomedical Engineering and Technology, Chinese Academy of Sciences, Suzhou 215163, China.*

† Electronic Supplementary Information (ESI) available: Related spectra. See DOI: 10.1039/b000000x/

1. D. Wencel, T. Abel and C. McDonagh, *Anal. Chem.*, 2014, **86**, 15-29.
2. J. Han and K. Burgess, *Chem. Rev.*, 2010, **110**, 2709-2728.
3. X. Lv, J. Liu, Y. Liu, Y. Zhao, Y.-Q. Sun, P. Wang and W. Guo, *Chem. Commun.*, 2011, **47**, 12843-12845.
4. W. Zhang, B. Tang, X. Liu, Y. Liu, K. Xu, J. Ma, L. Tong and G. Yang, *Analyst*, 2009, **134**, 367-371.
5. M. Tian, X. Peng, J. Fan, J. Wang and S. Sun, *Dyes Pigments*, 2012, **95**, 112-115.
6. J. Fan, C. Lin, H. Li, P. Zhan, J. Wang, S. Cui, M. Hu, G. Cheng and X. Peng, *Dyes Pigments*, 2013, **99**, 620-626.
7. R. Sun, X.-D. Liu, Z. Xun, J.-M. Lu, Y.-J. Xu and J.-F. Ge, *Sensor Actuat. B-Chem.*, 2014, **201**, 426-432.
8. L. Yuan, W. Lin, K. Zheng, L. He and W. Huang, *Chem. Soc. Rev.*, 2013, **42**, 622-661.
9. X.-D. Liu, Y. Xu, R. Sun, Y.-J. Xu, J.-M. Lu and J.-F. Ge, *Analyst*, 2013, **138**, 6542-6550.
10. B. Tang, X. Liu, K. Xu, H. Huang, G. Yang and L. An, *Chem. Commun.*, 2007, 3726-3728.
11. B. Tang, F. Yu, P. Li, L. Tong, X. Duan, T. Xie and X. Wang, *J. Am. Chem. Soc.*, 2009, **131**, 3016-3023.
12. Y. Tian, F. Su, W. Weber, V. Nandakumar, B. R. Shumway, Y. Jin, X. Zhou, M. R. Holl, R. H. Johnson and D. R. Meldrum, *Biomaterials*, 2010, **31**, 7411-7422.
13. Q.-J. Ma, H.-P. Li, F. Yang, J. Zhang, X.-F. Wu, Y. Bai and X.-F. Li, *Sensor Actuat. B-Chem.*, 2012, **166-167**, 68-74.
14. T. Jokic, S. M. Borisov, R. Saf, D. A. Nielsen, M. Kühl and I. Klimant, *Anal. Chem.*, 2012, **84**, 6723-6730.
15. N. Boens, W. Qin, M. Baruah, W. M. De Borggraeve, A. Filarowski, N. Smisdom, M. Ameloot, L. Crovetto, E. M. Talavera and J. M. Alvarez-Pez, *Chem. -Eur. J.*, 2011, **17**, 10924-10934.
16. W. Liu, R. Sun, J.-F. Ge, Y.-J. Xu, Y. Xu, J.-M. Lu, I. Itoh and M. Ihara, *Anal. Chem.*, 2013, **85**, 7419-7425.
17. H. Zhu, J. Fan, Q. Xu, H. Li, J. Wang, P. Gao and X. Peng, *Chem. Commun.*, 2012, **48**, 11766-11768.

18. L. Fan, Y. J. Fu, Q. L. Liu, D. T. Lu, C. Dong and S. M. Shuang, *Chem. Commun.*, 2012, **48**, 11202-11204.
19. R. Sun, W. Liu, Y.-J. Xu, J.-M. Lu, J.-F. Ge and M. Ihara, *Chem. Commun.*, 2013, **49**, 10709-10711.
20. T. Myochin, K. Kiyose, K. Hanaoka, H. Kojima, T. Terai and T. Nagano, *J. Am. Chem. Soc.*, 2011, **133**, 3401-3409.
21. H. He and D. K. Ng, *Org. Biomol. Chem.*, 2011, **9**, 2610-2613.
22. E. Deniz, G. C. Isbasar, O. A. Bozdemir, L. T. Yildirim, A. Siemiarczuk and E. U. Akkaya, *Org. Lett.*, 2008, **10**, 3401-3403.
23. Y. Tang, Y. Liu and A. Cao, *Anal. Chem.*, 2012, **85**, 825-830.
24. Y. Tang, L. Zhen, J. Liu and J. Wu, *Anal. Chem.*, 2013, **85**, 2787-2794.
25. B. C. Thompson, O. Winther-Jensen, B. Winther-Jensen and D. R. MacFarlane, *Anal. Chem.*, 2013, **85**, 3521-3525.
26. C. R. Schroder, B. M. Weidgans and I. Klimant, *Analyst*, 2005, **130**, 907-916.
27. U. C. Saha, K. Dhara, B. Chattopadhyay, S. K. Mandal, S. Mondal, S. Sen, M. Mukherjee, S. van Smaalen and P. Chattopadhyay, *Org. Lett.*, 2011, **13**, 4510-4513.
28. H. El Ouazzani, S. Dabos-Seignon, D. Gindre, K. Iliopoulos, M. Todorova, R. Bakalska, P. Penchev, S. Sotirov, T. Kolev, V. Serbezov, A. Arbaoui, M. Bakasse and B. Sahraoui, *J. Phys. Chem. C*, 2012, **116**, 7144-7152.
29. J. M. Hales, J. Matichak, S. Barlow, S. Ohira, K. Yesudas, J. L. Bredas, J. W. Perry and S. R. Marder, *Science*, 2010, **327**, 1485-1488.
30. M. T. Spitler and B. A. Parkinson, *Accounts. Chem. Res.*, 2009, **42**, 2017-2029.
31. J.-T. Miao, X.-Z. Wu, R. Sun, Y.-L. Song and J.-F. Ge, *Dyes Pigments.*, 2014, **105**, 41-46.
32. M. Guillaume and B. Champagne, *Phys. Chem. Chem. Phys.*, 2005, **7**, 3284-3289.
33. K. C. Hannah and B. A. Armitage, *Accounts. Chem. Res.*, 2004, **37**, 845-853.
34. C. Flors, *Biopolymers.*, 2011, **95**, 290-297.
35. N. I. Shank, H. H. Pham, A. S. Waggoner and B. A. Armitage, *J. Am. Chem. Soc.*, 2013, **135**, 242-251.
36. Z. Zhang and S. Achilefu, *Org. Lett.*, 2004, **6**, 2067-2070.
37. X. Peng, F. Song, E. Lu, Y. Wang, W. Zhou, J. Fan and Y. Gao, *J. Am. Chem. Soc.*, 2005, **127**, 4170-4171.
38. C. A. Bertolino, G. Caputo, C. Barolo, G. Viscardi and S. Coluccia, *J. Fluoresc.*, 2006, **16**, 221-225.
39. S. P. Wang, W. J. Deng, D. Sun, M. Yan, H. Zheng and J. G. Xu, *Org. Biomol. Chem.*, 2009, **7**, 4017-4020.
40. Q. Han, Z. Shi, X. Tang, L. Yang, Z. Mou, J. Li, J. Shi, C. Chen, W. Liu, H. Yang and W. Liu, *Org. Biomol. Chem.*, 2014, **12**, 5023-5030.
41. J. Han, A. Loudet, R. Barhoumi, R. C. Burghardt and K. Burgess, *J. Am. Chem. Soc.*, 2009, **131**, 1642-1643.
42. R. A. Rogers, A. R. Rodier, J. A. Stanley, N. A. Douglas, X. Li and W. J. Brittain, *Chem. Commun.*, 2014, **50**, 3424-3426.
43. A. Mishra, R. K. Behera, P. K. Behera, B. K. Mishra and G. B. Behera, *Chem. Rev.*, 2000, **100**, 1973-2012.
44. D. Plażuk, I. Janowska, A. Kłys, A. Hameed and J. Zakrzewski, *Synthetic. Commun.*, 2003, **33**, 381-385.
45. R. M. C. Dawson, D. C. Elliot, W. H. Elliot and K. M. Jones, *Data for Biochemical Research*, 3rd edn., Oxford Science Publ., 1986.
46. F. Doria, M. Nadai, G. Sattin, L. Pasotti, S. N. Richter and M. Freccero, *Org. Biomol. Chem.*, 2012, **10**, 3830-3840.
47. F. Song, X. Peng, E. Lu, Y. Wang, W. Zhou and J. Fan, *Tetrahedron Lett.*, 2005, **46**, 4817-4820.
48. Y. Chen, J. Zhao, H. Guo and L. Xie, *J. Org. Chem.*, 2012, **77**, 2192-2206.
49. D. H. Zhou, M. M. Li and L. L. Cui, *Acta Phys-chim. Sin.*, 2013, **29**, 1453-1460.
50. M. J. Frisch, G. W. Trucks, H. B. Schlegel, G. E. Scuseria, M. A. Robb, J. R. Cheeseman, G. Scalmani, V. Barone, B. Mennucci, G. A. Petersson, H. Nakatsuji, M. Caricato, X. Li, H. P. Hratchian, A. F. Izmaylov, J. Bloino, G. Zheng, J. L. Sonnenberg, M. Hada, M. Ehara, K. Toyota, R. Fukuda, J. Hasegawa, M. Ishida, T. Nakajima, Y. Honda, O. Kitao, H. Nakai, T. Vreven, J. A. Montgomery, J. Peralta, J. E. , F. Ogliaro, M. Bearpark, J. J. Heyd, E. Brothers, K. N. Kudin, V. N. Staroverov, T. Keith, R. Kobayashi, J. Normand, K. Raghavachari, A. Rendell, J. C. Burant, S. S. Iyengar, J. Tomasi, M. Cossi, N. Rega, J. M. Millam, M. Klene, J. E. Knox, J. B. Cross, V. Bakken, C. Adamo, J. Jaramillo, R. Gomperts, R. E. Stratmann, O. Yazyev, A. J. Austin, R. Cammi, C. Pomelli, J. W. Ochterski, R. L. Martin, K. Morokuma, V. G. Zakrzewski, G. A. Voth, P. Salvador, J. J. Dannenberg, S. Dapprich, A. D. Daniels, O. Farkas, J. B. Foresman, J. V. Ortiz, J. Cioslowski and D. J. Fox, Gaussian, Inc., Wallingford CT, 2010.
51. J. M. G. Cowie and P. M. Toporowski, *Can. J. Chem.*, 1961, **39**, 2240-2243.
52. C. Fruit, A. Turck, N. Plé, L. Mojovic and G. Quéguiner, *Tetrahedron*, 2001, **57**, 9429-9435.
53. L. Chausset-Boissarie, R. Arvai, G. R. Cumming, C. Besnard and E. P. Kundig, *Chem. Commun.*, 2010, **46**, 6264-6266.
54. M. Panigrahi, S. Dash, S. Patel and B. K. Mishra, *Tetrahedron*, 2012, **68**, 781-805.

## Graphical abstract

The indolium-phenol based tetramethylene hemicyanine has colorimetric and ratiometric optical responses under acidic and basic conditions.